Earth and Planetary Science Letters 357–358 (2012) 298–307

Contents lists available at SciVerse ScienceDirect

Earth and Planetary Science Letters

journal homepage: www.elsevier.com/locate/epsl

Origin of isotopic heterogeneity in the solar nebula by thermal processing and mixing of nebular dust

Christoph Burkhardt [a,*], Thorsten Kleine [b], Nicolas Dauphas [c], Rainer Wieler [a]

[a] Institute of Geochemistry and Petrology, Clausiusstrasse 25, ETH Zurich, CH-8092 Zurich, Switzerland
[b] Institut für Planetologie, Westfälische Wilhelms-Universität Münster, Wilhelm Klemm-Strasse 10, D-48149 Muenster, Germany
[c] Origins Laboratory, Department of the Geophysical Sciences and Enrico Fermi Institute, The University of Chicago, 5734 South Ellis Avenue, Chicago, IL 60637, USA

ARTICLE INFO

Article history:
Received 31 March 2012
Received in revised form
14 September 2012
Accepted 28 September 2012
Editor: T. Elliot

Keywords:
Mo isotopes
W isotopes
nucleosynthesis
meteorites
solar nebula

ABSTRACT

We have investigated Mo and W isotope compositions in acid leachates and an insoluble residue from the Murchison carbonaceous chondrite. The new data reveal variable enrichments of *s*- and *r*-process isotopes and demonstrate that several isotopically diverse presolar components are present in Murchison. The insoluble residue is enriched in *s*-process Mo and W, evidently due to the enrichment of presolar SiC grains. In contrast, Mo and W released by leaching with weak acids are depleted in *s*-process isotopes, most likely reflecting the isotope composition of the homogenized portion of the protosolar nebula. The Mo and W isotope compositions of the different leach steps are broadly correlated as expected from *s*-process nucleosynthesis theory, indicating that Mo and W are presumably hosted in the same carriers. However, at the bulk meteorite scale, no nucleosynthetic W isotope anomalies have been identified (except for IVB iron meteorites) in spite of large Mo isotope heterogeneities among the same samples. This decoupling of Mo and W isotopes in bulk meteorites may reflect physical mixing of varying proportions of isotopically diverse presolar components with a "normal" solar nebula component. Due to the high W/Mo ratio and near-terrestrial W isotope composition of the latter, such mixing has no measurable effect on W isotopes, but results in large Mo isotope variations. Alternatively, thermal processes within the solar nebula imparted Mo isotope heterogeneity on an initially homogeneous mixture of presolar dust, while W was not affected. Removal of volatile Mo oxides during the thermal destruction of fragile presolar components would have created isotopically heterogeneous reservoirs of nebular dust. Accretion of meteorite parent bodies from such variably processed dust would thus result in Mo isotope heterogeneities at the bulk meteorite scale. Other elements such as Os and W were not or only slightly affected because they were more refractory during thermal processing and, therefore, remained isotopically homogeneous. Thermal processing of presolar dust within the solar nebula can thus account for both isotope heterogeneities observed for some elements *and* the lack of such isotopic heterogeneity for other elements.

1. Introduction

Bulk meteorites exhibit small but resolvable mass-independent isotopic anomalies in various elements (*e.g.*, Ca, Ti, Cr, Ni, Mo, Ru, Nd, Sm) (Chen et al., 2011a, Niemeyer and Lugmair, 1984; Trinquier et al., 2007; Regelous et al., 2008; Dauphas et al., 2002b; Burkhardt et al., 2011; Chen et al., 2010; Andreasen and Sharma, 2006) that are commonly interpreted as reflecting incomplete homogenization of isotopically diverse presolar dust in the solar nebula. In contrast, uniform and terrestrial isotopic compositions were reported for some other elements (*e.g.*, Os, Hf) (Brandon et al., 2005; Sprung et al., 2010; Yokoyama et al., 2007; Walker, 2012), indicating that the presolar carriers of at least these elements were well mixed in the nebula. These contrasting isotopic characteristics of different elements are poorly understood but are key for constraining the origin of nucleosynthetic isotope anomalies in bulk meteorites.

Several models have been proposed to account for the isotopic heterogeneity observed at the bulk meteorite scale. It has been suggested that this is a primordial feature of the solar nebula inherited from a heterogeneous presolar molecular cloud core (Clayton, 1982; Dauphas et al., 2002b), or caused by the late injection of freshly synthesized matter into the nebula (Trinquier et al., 2007). Furthermore, processes within the solar nebula, such as separation of dust grains of different types (*e.g.*, silicates and sulfides) (Regelous et al., 2008), size-sorting (Dauphas et al., 2010) or selective destruction of thermally labile presolar components

* Corresponding author. Tel.: +41 44 63 26455; fax: +41 44 63 21827.
E-mail address: burkhardt@erdw.ethz.ch (C. Burkhardt).

0012-821X/$ - see front matter © 2012 Elsevier B.V. All rights reserved.
http://dx.doi.org/10.1016/j.epsl.2012.09.048

(Trinquier et al., 2009), may have been important in generating isotopic anomalies in bulk meteorites. For fluid-mobile elements, the selective destruction of presolar grains during parent body processes may also have played a role in modifying the isotopic composition of chondrites (Yokoyama et al., 2011). Models that invoke nebular or parent-body processes for generating the isotopic heterogeneity observed among bulk meteorites can potentially account for the disparate isotope systematics of different elements because elemental fractionation may have occurred during such processes. However, the specific behavior of different elements during nebular or parent-body processes is not known, nor has a systematic study been conducted comparing isotopic variations in elements that may have responded differently during nebular or parent-body processing.

Here we present the first Mo isotopic data for acid leachates and an acid-resistant residue of the Murchison chondrite. Aliquots from the same leachates were also investigated for W (Burkhardt et al. 2012) and Os isotope compositions (Reisberg et al., 2009). Combined with available Mo, W and Os isotope data for bulk meteorites, the Mo and W leachate data are used to assess the origin of both, heterogeneous Mo isotopes in bulk meteorites, *and* near-uniform Os and W isotope compositions in the same bulk samples.

2. Analytical methods

The Mo isotopic measurements were performed on aliquots from six different samples obtained by the sequential dissolution of a ~16.5 g whole-rock powder of the carbonaceous chondrite Murchison. The dissolution was performed at the University of Chicago using the following sequence (see Reisberg et al. (2009)):

L1: 9 M HAc (acetic acid), 1 day, 20 °C;
L2: 4.7 M HNO_3, 5 days, 20 °C;
L3: 5.5 M HCl, 1 day, 75 °C;
L4: 13 M HF/3 M HCl, 1 day, 75 °C;
L5: 13 M HF/6 M HCl, 3 days, 150 °C;
L6: insoluble residue.

After drying down, the aliquots of samples L1–L5 were treated with aqua regia, dried and then re-dissolved in 6 M HCl. To completely dissolve all presolar grains remaining in the insoluble residue (L6), this sample was first fused by a CO_2 laser under a reducing atmosphere (see Burkhardt et al. (2011)), and then digested in HNO_3–HF–$HClO_4$. After drying down, sample L6 was completely dissolved in 6 M HCl. Small aliquots of all samples were spiked with a mixed ^{97}Mo–^{180}Hf–^{183}W tracer for concentration measurements by isotope dilution. Purification of Mo (+W, Hf) from the sample matrix was performed by ion exchange chromatography in HCl–HF media (Burkhardt et al., 2011; Kleine et al., 2004). Total procedural Mo blanks were ~400 pg for the unspiked and ~48 pg for the spiked aliquots and no blank correction was required. The blank introduced by the leaching procedure itself could not be assessed, but is expected to be small because only ultra-pure acids and Milli-Q water was used (see Reisberg et al. (2009)).

Molybdenum isotope measurements on the unspiked aliquots were performed using the large-geometry *Nu Plasma* 1700 MC-ICP-MS at ETH Zürich, equipped with a Cetac Aridus II desolvating nebulizer (for details see Burkhardt et al. (2011)). Molybdenum isotopic compositions were typically measured at ion beam intensities of ~$2–3 \times 10^{-11}$ A on ^{96}Mo, which was obtained for a ~75 ppb Mo solution at an uptake rate of ~100 µl/min. Due to its low Mo content, sample L5 was measured at ~5×10^{-12} A on ^{96}Mo. The Mo isotopic data are reported as ε^{i}Mo, which is the part per 10^4 deviation of the ^{i}Mo/^{96}Mo ratio from the mean of the two bracketing runs of the terrestrial standard. The external reproducibility of the ~75 ppb Mo standard (Alfa Aesar Mo) was ±0.75 ε^{92}Mo, ±0.50 ε^{94}Mo, ±0.41 ε^{95}Mo, ±0.23 ε^{97}Mo and ±0.44 ε^{100}Mo. Corrections for isobaric interferences of Zr and Ru on Mo masses were smaller than 2 ε for all samples and assumed terrestrial isotopic composition for these elements. Instrumental mass bias was corrected using the exponential law and ^{98}Mo/^{96}Mo = 1.453171 (Lu and Masuda, 1994). This normalization is best suited to resolve nucleosynthetic anomalies (Burkhardt et al., 2011).

3. Results

The concentrations of Mo and W in the various leachate fractions and the insoluble residue (Table 1) were calculated by dividing the quantity of Mo or W in the leachates by the total mass of the Murchison sample. While the majority of the Mo (~68%) is released in the second leaching step, the largest fraction of W (~48%) is contained in leaching step 4 (Fig. 1). The total Mo and W concentrations, calculated as the sum of the concentrations determined for each leaching step, are in good agreement with results for bulk rock analyses (1.15 ppm Mo here *vs.* 1.27 ppm in Burkhardt et al. (2011); 123 ppb W here *vs.* 130 ppb in Kleine et al. (2004)), indicating that all components of Murchison were digested in the leaching procedure.

The Mo isotopic data are listed in Table 1 and plotted on ε^{i}Mo versus atomic mass ^{i}Mo (Fig. 2) and ε^{92}Mo versus ε^{i}Mo diagrams (Fig. 3). All samples exhibit large Mo isotopic anomalies ranging from +30.5 ε^{92}Mo for L1 (HAc leachate) to −79.3 ε^{92}Mo for L6 (insoluble residue). The weighted average of the leachates yields ε^{92}Mo = 4.39 ± 0.53, slightly lower than ε^{92}Mo = 6.44 ± 0.39 reported for bulk Murchison (Burkhardt et al., 2011). This difference may reflect sample heterogeneity or loss of a small fraction of isotopically anomalous Mo from the leachates. The Mo isotopic compositions of the different leaching steps are consistent with deficits (L1–L3) and excesses (L4–L6) in *s*-process isotopes. A deficit in *s*-process Mo relative to terrestrial Mo leads to positive ε^{i}Mo values (for normalization to ^{98}Mo/^{96}Mo) and is characterized by a *w*-shaped pattern in a ε^{i}Mo–^{i}Mo diagram. Conversely, an *s*-excess results in negative ε^{i}Mo values and a corresponding *m*-shaped pattern (Burkhardt et al., 2011; Dauphas et al., 2002a). Note that a variable distribution of *r*-process Mo isotopes would result in different patterns, *i.e.*, an additional kink in ^{94}Mo (Burkhardt et al., 2011).

4. Presolar carrier phases of Mo and W isotope anomalies

4.1. Nature and origin of Mo isotope anomalies

The Mo isotopic data reveal large internal isotope variations and demonstrate that several presolar, isotopically diverse components are present in Murchison. A previous leaching experiment on the CI chondrite Orgueil revealed similar Mo isotope patterns, albeit of smaller magnitude (Dauphas et al., 2002a). The different magnitude of the isotope anomalies might be caused by the slightly different leaching procedures used in the two studies, but more likely is due to the higher degree of parent body alteration of Orgueil compared to Murchison. In ε^{92}Mo versus ε^{i}Mo diagrams (Fig. 3), the data for all the leaching steps plot along positive correlation lines that pass through the terrestrial Mo isotopic composition. Molybdenum isotopic data for acid leachates of Orgueil (Dauphas et al., 2002a) as well as a Ca, Al-rich inclusion (CAI) from Allende (A-ZH-5; a type A CAI characterized by

Table 1
Mo and W concentrations and isotopic compositions for leachates and bulk Murchison.

Sample	Procedure	N[a]	Mo ± 2σ (ng/g)	W ± 2σ (ng/g)	W/Mo ± 2σ	ε^{92}Mo[b] ± 2σ	ε^{94}Mo[b] ± 2σ	ε^{95}Mo[b] ± 2σ	ε^{97}Mo[b] ± 2σ	ε^{100}Mo[b] ± 2σ	ε^{183}W[c] ± 2σ
Murchison											
L1	9 M HAc 1day, 20 °C	1	48.98 ± 0.01	7.83 ± 0.20	0.160 ± 0.004	30.54 ± 0.75	24.14 ± 0.50	15.25 ± 0.41	7.78 ± 0.23	9.67 ± 0.44	3.62 ± 0.50
L2	4.7 M HNO_3, 5 days, 20 °C	5	784.37 ± 0.04	20.85 ± 0.36	0.027 ± 0.001	6.65 ± 0.36	5.17 ± 0.24	3.36 ± 0.07	1.73 ± 0.09	2.24 ± 0.25	0.99 ± 0.50
L3	5.5 M HCl, 1 day, 75 °C	4	213.30 ± 0.02	27.42 ± 0.39	0.129 ± 0.002	4.20 ± 0.42	3.38 ± 0.35	2.20 ± 0.14	1.11 ± 0.08	1.32 ± 0.27	0.59 ± 0.50
L4	13 M HF 3 M HCl, 1 day, 75 °C	1	74.56 ± 0.02	59.43 ± 0.76	0.80 ± 0.01	−6.15 ± 0.75	−5.01 ± 0.50	−2.33 ± 0.41	−1.48 ± 0.23	−1.38 ± 0.44	0.38 ± 0.28
L5	13 M HF 6 M HCl, 3 days, 150 °C	1	8.30 ± 0.01	3.00 ± 0.20	0.36 ± 0.02	−21.23 ± 1.27	−17.73 ± 1.27	−9.98 ± 0.58	−5.46 ± 0.62	−5.85 ± 0.61	−1.22 ± 1.38
L6	insoluble residue, Laser fused	1	24.07 ± 0.01	4.50 ± 0.23	0.19 ± 0.01	−79.30 ± 0.75	−64.42 ± 0.50	−38.19 ± 0.41	−20.75 ± 0.23	−25.48 ± 0.44	−15.28 ± 0.50
Total (conc.) or wt. ave. (ratios)			1153.6 ± 0.1	123.0 ± 1.0	0.107 ± 0.001	4.39 ± 0.43	3.37 ± 0.30	2.32 ± 0.13	1.14 ± 0.11	1.51 ± 0.28	0.12 ± 0.42
Bulk Murchison[d]		7	1145 ± 10	133.6[e] ± 0.3	0.117 ± 0.001	6.44 ± 0.39	4.82 ± 0.20	3.17 ± 0.16	1.66 ± 0.14	2.28 ± 0.22	0.08 ± 0.50

[a] N = number of analyses.
[b] $\varepsilon^{i}Mo = [(^{i}Mo/^{96}Mo)_{sample}/(^{i}Mo/^{96}Mo)_{standard} - 1] \times 10^4$ for internal normalization to $^{98}Mo/^{96}Mo = 1.453171$. For samples measured once, errors are estimated by the standard deviation (2 SD) from repeated analysis of the terrestrial standard. For samples measured more than once uncertainties were calculated using $\sigma t_{0.95,n-1}/\sqrt{n}$.
[c] W isotope data from Burkhardt et al. (2012); $\varepsilon^{183}W = [(^{183}W/^{184}W)_{sample}/(^{183}W/^{184}W)_{standard} - 1] \times 10^4$ for internal normalization to $^{186}W/^{184}W = 0.92767$.
[d] Bulk Murchison Mo data from Burkhardt et al. (2011).
[e] W concentration from Kleine et al. 2004.

Fig. 1. Fraction of Mo and W released in the different leaching steps.

a large deficit in *s*-process Mo) and bulk meteorites (Burkhardt et al., 2011) also plot on these correlation lines. The ε^{92}Mo–ε^{i}Mo correlation lines are consistent with variable proportions of *s*-process Mo, as calculated using the *s*-process abundances of the stellar model of Arlandini et al. (1999) or data for mainstream SiC grains (Nicolussi et al., 1998).

The measured slopes of the ε^{92}Mo–ε^{i}Mo correlation lines compare well to those calculated using the stellar model or SiC data. For the ε^{92}Mo–ε^{94}Mo correlation the slopes are 0.80 ± 0.02 (from the leachates), 0.83 ± 0.03 (from the stellar model) and 0.79 ± 0.02 (from SiC). For the other Mo isotopes the slopes of the correlations lines with ε^{92}Mo are 0.49 ± 0.01, 0.38 ± 0.02 and 0.47 ± 0.01 for ε^{95}Mo, 0.26 ± 0.01, 0.20 ± 0.01 and 0.20 ± 0.01 for ε^{97}Mo, and 0.31 ± 0.02, 0.32 ± 0.10 and 0.29 ± 0.02 for ε^{100}Mo, respectively. The slight deviation for ε^{95}Mo and ε^{97}Mo between the stellar model and the leachate data suggest that the *s*-process yields for ^{95}Mo and ^{97}Mo might be lower than predicted by the stellar model. The offset between the leachate and SiC data in the ε^{92}Mo–ε^{97}Mo correlation (Fig. 3c) could reflect *s*-process variability in the SiC grains, nuclear field shift effects (Fuji et al., 2006) or radiogenic ^{97}Mo variations from ^{97}Tc-decay. The latter two possibilities can be excluded because all samples, including leachates and bulk meteorites, plot on a single well-defined ε^{97}Mo–ε^{92}Mo correlation, despite their very different cosmochemical histories and Tc(Ru,Re)/Mo ratios. Lugaro et al. (2003) showed that the *s*-process yield for ^{97}Mo varies substantially with stellar mass and corresponding size of the ^{13}C-pocket. However, this is unlikely to explain the slight mismatch between the SiC and leachate data, because leach step 6, which presumably is enriched in SiC (see below), plots on the same line as the other leachates. It is noteworthy that forcing the ^{97}Mo vs. ^{92}Mo regression of the SiC data (Nicolussi et al., 1998) through the origin, or using only single grain SiC data, would result in a lower *s*-process yield for ^{97}Mo, which would be more consistent with the leachate data.

Overall the observed Mo isotope variations among bulk meteorites and meteorite components (except type B CAI (Burkhardt et al., 2011)) can be explained by a heterogeneous distribution of one or more carriers of *s*-process Mo. At least two components must be present to account for the observed

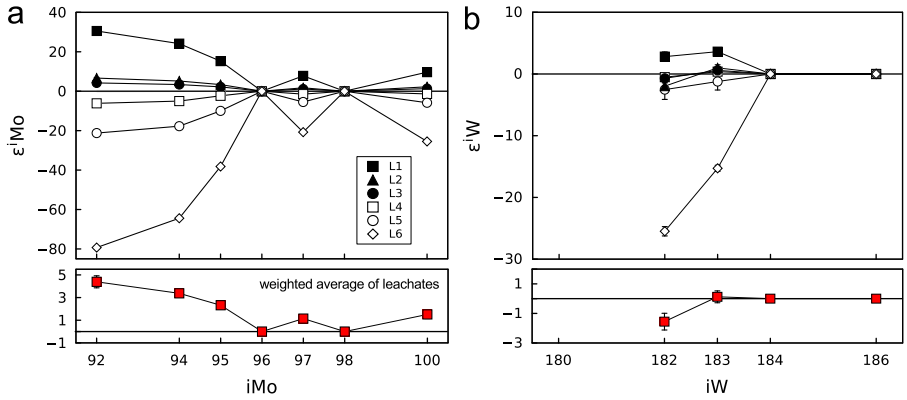

Fig. 2. Mo and W isotope data for the different leach steps of Murchison. (a) Mo isotopic data normalized to $^{98}Mo/^{96}Mo$. (b) W isotopic data normalized to $^{186}W/^{184}W$ (Burkhardt et al., 2012). Leachates L1–L3 are consistent with a deficit in *s*-process isotopes relative to terrestrial Mo and W, while leachates L4-L6 exhibit *s*-enrichments. The weighted average of the different leach steps shows a resolvable *s*-deficit for Mo, but no resolvable anomalies in non-radiogenic W isotopes.

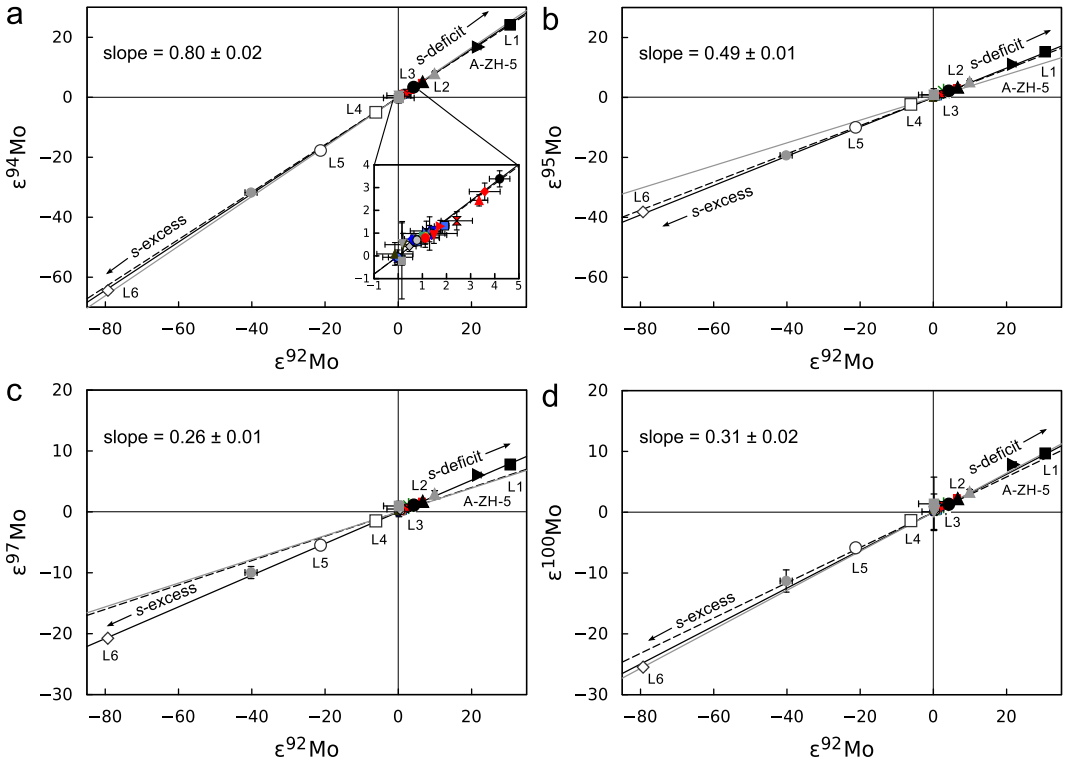

Fig. 3. ε^{92}Mo–ε^{i}Mo plots for Murchison leachates. Symbols are as in Fig. 2. Also plotted are data for different leach steps of Orgueil (grey symbols; Dauphas et al., 2002a), for CAI A-ZH-5, and for bulk meteorites (see inset of a) (Burkhardt et al., 2011). Black lines are regressions including data for the leachates, bulk meteorites, and CAI A-ZH-5. The regressions represent mixing lines between terrestrial Mo and a presumed *s*-process component. These calculated mixing lines are in excellent agreement with *s*-process compositions predicted in the stellar model of Arlandini et al. (1999) (grey lines), and with measurements for presolar SiC grains (dashed-line) (Nicolussi et al. 1998). For ^{95}Mo and ^{97}Mo, the predictions of the stellar model deviate slightly from the Mo isotope data of the leachates, indicating that the cross sections of these two Mo isotopes may need slight adjustment. The SiC data deviate slightly from the leachate data for ^{97}Mo. For discussion see text.

co-variation in ε^{92}Mo versus ε^{i}Mo plots. These were termed Mo-*w* and Mo-*m* by Dauphas et al. (2002a) and are characterized by a deficit in *s*-process Mo (Mo-*w*) and complementary excess in *s*-process Mo (Mo-*m*). Dauphas et al. (2002a) noted that Mo-*w* cannot be attributed to a specific nucleosynthetic carrier phase, because a nucleosynthetic process is unlikely to produce *p*- and *r*-process nuclides in exactly solar proportions. The Mo-*w* pattern, therefore, most likely represents a "homogenized" nebula component, which is depleted in *s*-process Mo relative to the Earth.

Presolar mainstream SiC and graphite grains contain almost pure *s*-process Mo (Nicolussi et al., 1998) and, therefore, are viable carriers of the Mo-*m* component. The insoluble residue of Murchison remaining after acid leaching is enriched in presolar SiC grains, so that the strong enrichment in *s*-process Mo isotopes of the insoluble residue (L6) almost certainly reflects the signature of SiC. It is less clear, however, as to whether SiC also is the carrier responsible for generating the observed Mo isotopic heterogeneity at the bulk meteorite scale. For instance, the leachate data show that phases enriched in *s*-process Mo are already released during leaching with HF–HCl (L4, L5), which is not expected to dissolve SiC or graphite. This might indicate that yet unidentified presolar phases (*e.g.*, silicates or oxides) are additional carriers of *s*-process Mo. Alternatively, the *s*-process enriched signatures of the HF–HCl leachates result from leaching Mo from surfaces of SiC grains, which are etched by exposure to acids (Macke et al., 1999; Bernatowicz et al., 2000).

The progressive release of *s*-process Mo from SiC grains during differential dissolution could account for the observation that with increasing acid strength the isotopic composition of the released Mo becomes richer in *s*-process Mo. Alternatively, this observation may reflect the presence of several distinct carriers of *s*-process Mo, which would need to have very similar Mo isotopic signatures because all the leachates plot along a two-component mixing line. The formation of different presolar grain types in AGB stars, the dominant site of the *s*-process, depends on the age of the star. At the start of the *s*-process the C/O ratio in the star is low, allowing the formation of oxide and silicate grains, while at later times the C/O ratio is higher, favoring the condensation of carbides and graphite. The *s*-process composition of the products synthesized in the different C/O regimes during stellar evolution might be different, because neutron reaction paths can change during AGB-star evolution (Reisberg et al., 2009). However, for Mo the changes in the *s*-process compositions in different C/O regimes appear to be rather small (Lugaro et al., 2003), such that the Mo isotopic data for the leachates allow for the presence of more than one *s*-process carrier.

4.2. Comparison of nucleosynthetic Mo and W isotope anomalies in acid leachates

The same leachates examined here for Mo isotopes have also been analyzed for their W isotopic compositions (Burkhardt et al., 2012). The ε^{183}W data of all samples [$\{\varepsilon^{183}W=(^{183}W/^{184}W)_{sample}/(^{183}W/^{184}W)_{standard}-1\}\times 10^4$] normalized to ^{186}W/^{184}W are given in Table 1 and plotted in Fig. 2b. The W isotopic compositions of the leachates are in reasonable agreement with predictions of the stellar *s*-process model (Arlandini et al., 1999). While the leachates L1-3 show an *s*-deficit (or *r*-excess), L5 and L6 exhibit an *s*-excess (*r*-deficit). The nucleosynthetic W isotope anomalies in the different leach steps, therefore, most likely reflect a heterogeneous distribution of *s*-process W in Murchison (Burkhardt et al., 2012).

As shown in Fig. 4a, the Mo and W isotopic anomalies in the different leaching steps of Murchison are broadly correlated, as is expected for a variable distribution of *s*-process isotopes. The ε^{183}W–ε^{92}Mo correlation line in Fig. 4a was calculated using the mixing equation for internally normalized isotope ratios (Dauphas et al., 2004), the *s*-process abundances of Mo and W isotopes from the stellar *s*-process model (Arlandini et al., 1999) and a solar W/Mo ratio as follows:

$$\varepsilon^{183}W=\frac{\varrho^{183}W-\varrho^{186}W\mu^{183}W}{\varrho^{92}Mo-\varrho^{98}Mo\mu^{92}Mo}c\times\varepsilon^{92}Mo$$

where ρ^{i}W and ρ^{i}Mo represent the *s*-process composition normalized to the terrestrial composition,

$$\varrho^{i}W=\frac{\left(\frac{^{i}W}{^{184}W}\right)_s}{\left(\frac{^{i}W}{^{184}W}\right)_{terr}}-1\quad \varrho^{i}Mo=\frac{\left(\frac{^{i}Mo}{^{96}M}o\right)_s}{\left(\frac{^{i}Mo}{^{96}M}o\right)_{terr}}-1$$

μ^{i}W and μ^{i}Mo are the mass differences relative to the normalizing pairs,

$$\mu^{183}W=\left(\frac{183-184}{186-184}\right)\mu^{92}Mo=\left(\frac{92-96}{98-96}\right)$$

and *c* is the curvature coefficient of the mixing relationship,

$$c=\frac{\left(^{184}W/^{96}Mo\right)_s}{\left(^{184}W/^{96}Mo\right)_{solar}}$$

The slope of the ε^{183}W–ε^{92}Mo correlation line depends on the curvature coefficient and thus varies with different Mo/W ratios in the individual leachates (the sign of the slope will not change, however (Dauphas et al., 2004; Burkhardt et al., 2011)). The reasonable agreement of the correlation line in Fig. 4a with the Mo and W isotopic anomalies for the different Murchison leachates and CAI A-ZH-5 (Burkhardt et al., 2008; 2011) indicates that the Mo and W isotope anomalies are probably hosted in the same carriers.

5. Origin of nucleosynthetic isotope anomalies in bulk meteorites

Fig. 4b shows that the Mo isotope anomalies in bulk meteorites of up to $\sim+6$ ε^{92}Mo would correspond to nucleosynthetic W isotope variations of up to $\sim+1$ ε^{183}W, provided that the Mo and W isotope variations reflect a heterogeneous distribution of *s*-process-rich and -poor endmembers having approximately solar Mo/W ratios. However, bulk meteorites do not exhibit resolvable anomalies in ε^{183}W at the ±0.1 ε-unit level (*e.g.*, Kleine et al., 2004; 2005; Qin et al., 2008b; Scherstén et al., 2006). The only exception are IVB iron meteorites, which show a small anomaly of $\varepsilon^{183}W\approx+0.1$ (Qin et al., 2008a; Kruijer et al., 2012). However, this anomaly is smaller than $\varepsilon^{183}W\approx+0.25$ that would be expected based on the ε^{183}W–ε^{92}Mo correlation line defined by the acid leachates from Murchison (Fig. 4b). Thus, although the leachate data strongly suggest that the Mo and W isotope anomalies are hosted in the same carriers, these isotope anomalies are *decoupled* at the bulk meteorite scale. This decoupling may either reflect mixing of presolar carriers with different Mo/W ratios, or thermal processing of presolar dust that imparted Mo isotopic heterogeneity on an initially well-mixed solar nebula. These two possibilities are discussed in more detail in Sections 5.1 and 5.2.

5.1. Mixing of different presolar components

One possibility to explain the presence of correlated isotopic anomalies for Mo and W in Murchison leachates, and the lack of such a correlation at the bulk meteorite scale, is that this reflects variations in the Mo/W ratio of the *s*-rich and *s*-poor mixing endmembers. In epsilon–epsilon diagrams between different elements, binary mixing generally appears as linear because the isotopic anomalies considered are very close to one of the endmembers (*i.e.*, the very anomalous *s*-process endmember is strongly diluted by average solar system material). As a result, what is actually a curve appears as a straight line over this narrow field of view. The slope of the correlation line depends on the elemental ratio of each mixing endmember, *i.e.*, the curvature coefficient (see above).

The first three acid leachates as well as CAI A-ZH-5 plot on the theoretical ε^{183}W–ε^{92}Mo correlation (Fig. 4a and b). However, the other leachates depart from this trend, indicating that the *s*-rich and *s*-poor reservoirs tapped by the leaching procedure do not all have constant W/Mo ratios. Keeping the W/Mo ratio of the *s*-rich endmember constant, this departure can be explained if the solar nebula component in these leachates has a high W/Mo ratio so that the *s*-process W is masked by "normal" W, while *s*-process Mo is visible because it is less diluted. This is most obvious for leachate L4, which plots to the left of the theoretical ε^{183}W–ε^{92}Mo correlation line and is characterized by a high W/Mo of $\sim$0.8 (compared to a solar W/Mo $\sim$0.1). An intriguing feature of this leachate is that it contains the largest fraction of W ($\sim$48%) and is characterized by an almost normal (*i.e.*, terrestrial) W isotopic composition ($\varepsilon^{183}W=0.38\pm0.28$) but a large Mo isotope anomaly ($\varepsilon^{92}Mo=-6.15\pm0.75$). Admixture of material of the *s*-rich or *s*-poor endmembers with approximately solar W/Mo to this component, therefore, will only slightly affect its W isotopic composition while the effects on Mo isotopes are much more pronounced.

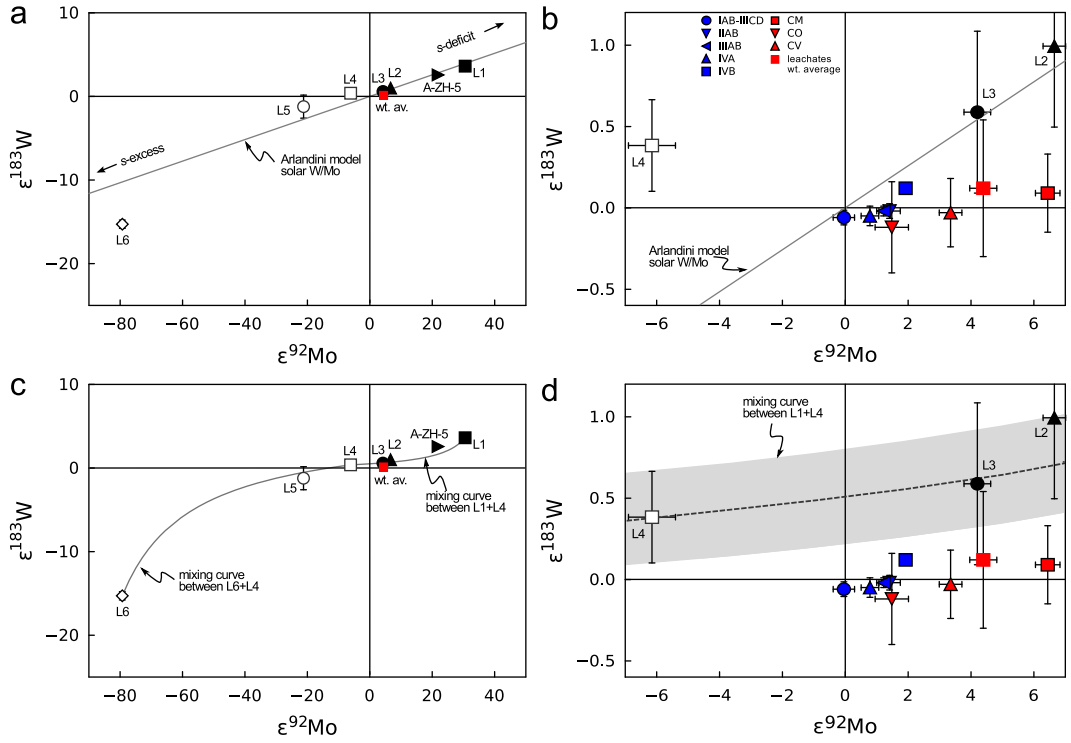

Fig. 4. ε^{183}W–ε^{92}Mo plots for Murchison leachates and bulk meteorites. Straight grey lines in (a) and (b) are mixing lines between terrestrial Mo and W and a presumed *s*-process component, calculated using the *s*-process composition of Arlandini et al. (1999). Grey lines in (c) and (d) represent mixing curves between L6 and L4, and between L4 and L1. The high W/Mo of L4 compared to L6 and L1 results in hyperbolic mixing curves. The Mo and W isotope anomalies in the leachates broadly follow the theoretical ε^{183}W–ε^{92}Mo correlation line calculated assuming solar W/Mo ratios (a), but bulk meteorites do not plot on this correlation line (b). (c) Leachates L5, L3 and L2 plot exactly on hyperbolic mixing curves between L6 and L4, and between L4 and L1, and bulk meteorites plot close to the calculated mixing line between L4 and L1 (d.). Bulk meteorite data from Burkhardt et al. (2011), Kleine et al. (2004) and Qin et al. (2008b). Width of the grey bar is defined by mixing calculations between the maximum uncertainties of L4 and L1.

In contrast to W, the major fraction of Mo (~68%) is released in leachate L2 (Fig. 1). This leachate is characterized by a very low W/Mo ratio of ~0.03 and a large Mo isotope anomaly of ε^{92}Mo ≈ 6.7, while its W isotopic composition is ε^{183}W ≈ 1. Due to its high Mo content and anomalous Mo isotopic composition, a heterogeneous distribution of a component like L2 would cause significant Mo isotope variations, but owing to its low W/Mo ratio the collateral effects on W isotopes would be much smaller. Overall it thus appears conceivable that mixing of distinct presolar components having non-solar W/Mo ratios controlled the distribution of W and Mo isotopic anomalies at the planetary scale and is responsible for the contrasting isotope signatures of the two elements in bulk meteorites.

To test this model, we have calculated mixing trajectories between leachates L4 and L6, and between L1 and L4 (Fig. 4c and d). An important observation from these calculations is that L2 and L3 plot on the mixing curve between L1 and L4, and L5 plots on the mixing curve between L6 and L4. Thus, mixing between L1, L4 and L6 can account for the Mo and W isotopic compositions of each of the different leach steps. Owing to the much higher W/Mo in L4 compared to L1 or L6, the mixing curves in ε^{183}W versus ε^{92}Mo diagrams are approximately horizontal close to the composition of L4, so that mixing does not induce W isotope heterogeneities, but results in significant Mo isotope variations (Fig. 4c and d). The mixing calculations, therefore, can successfully reproduce the disparate Mo and W isotope systematics observed at the bulk meteorite scale.

However, it is unclear as to whether the mixing model can also explain the terrestrial ε^{183}W of almost all bulk meteorites. Although leachates L2, L3 and L4 do not deviate much from the normal, terrestrial W isotopic composition, all of them have slightly positive ε^{183}W. Thus, using the nominal ε^{183}W values for the leachates L2 to L4 would predict resolvable positive ε^{183}W for all bulk meteorites, but these generally have ε^{183}W ≈ 0 (Fig. 4b and d). Thus, the mixing model can only account for the lack of nucleosynthetic W isotope anomalies in bulk meteorites, if the true ε^{183}W of leachate L4 is close to the lower error bound of the measured value. Another problem with the mixing model is that mixing between L1 and L4 falls short in reproducing the W/Mo ratios of L2 and L3, because both L1 and L4 have higher W/Mo than L2 and L3. This may indicate that L1 and L4 do not represent true endmember compositions or that the W/Mo ratios were fractionated during leaching or parent body alteration. To fully resolve these issues more precise W isotope data for acid leachates that tap the "normal" solar nebula component in primitive chondrites other than Murchison are needed.

In summary, the Mo isotopic anomalies in bulk meteorites may reflect the heterogeneous distribution of one or several presolar carriers of nucleosynthetic anomalies that were mixed with a "normal" solar nebula component characterized by high W/Mo and near-terrestrial ε^{183}W (such as in leachate L4), so that W isotope anomalies are largely masked by this normal component. In contrast, Mo isotopic anomalies are less diluted and, therefore, are visible at the bulk meteorite scale. If leachate L4 indeed represents the normal solar nebula component, the question arises as to how this component acquired its high, distinctly non-solar W/Mo ratio. This would imply a large-scale fractionation of Mo from W by nebular processes. As will be argued below, thermal processing of nebular dust may be one possibility for generating such large Mo/W fractionations.

5.2. Thermal processing of presolar dust

A second possibility to account for the decoupling of Mo and W isotopic anomalies in bulk meteorites and meteorite components

(as revealed by the acid leachates) is that the isotopic anomalies in bulk meteorites were produced by thermal processing of an initially homogeneous mixture of nebular dust consisting of isotopically diverse presolar components. Thermal processing of presolar dust has been suggested previously as a mechanism to account for the correlation of presolar grain abundances and bulk chemical composition in chondrites (Huss, 2004). In this model, it is argued that the distinct abundances of presolar grains in different classes of primitive chondrites reflect heating and thermal destruction of fragile presolar components to varying degrees in the solar nebula prior to parent body accretion (Huss et al., 2003; Huss, 2004). Such a selective destruction and partial evaporation of thermally labile presolar components might have induced isotopic heterogeneities in the nebular dust. At least some of the elements that became vaporized during thermal processing might have separated from nebular dust before they could recondense. The isotopic composition of the vaporized, removed component would reflect that of the thermally destructed material and, consequently, would be different from the average isotopic composition of the dust. The removal of isotopically anomalous material would, therefore, impart isotopic anomalies on the processed dust, complementary to the composition of the removed volatilized component. Trinquier et al. (2009) proposed such processes as the dominant mechanism causing Ti isotopic heterogeneities among bulk meteorites.

Thermal destruction and partial evaporation of presolar components acts differently on different elements and should thus be capable to decouple the isotopic systematics of different elements. As to whether elements can be vaporized and lost ultimately depends on the tendency of an element to enter the vapor phase during the thermal events. The decoupling of Mo and W isotopic anomalies in bulk meteorites and acid leachates, therefore, can be explained if during thermal processing of nebular dust Mo was preferentially evaporated and removed, while W was not affected. During evaporation under oxidizing conditions Mo becomes more volatile than W and could thus have been lost preferentially into the gas phase (Fegley and Palme, 1985). It is noteworthy that W is always less volatile than Mo, so that the Mo depletions are always larger than those in W (Fegley and Palme, 1985). The formation of volatile Mo oxides is thought to be responsible for the pronounced Mo depletions observed in some CAI. Most CAI also exhibit W depletions, but these are always smaller than those of Mo. The elemental Mo–W systematics of CAI, therefore, demonstrates that conditions prevailed in the solar nebula that led to a preferential loss of Mo, and a substantial fractionation of Mo from W.

We therefore propose that the presence of correlated Mo and W isotopic anomalies in the acid leachates of Murchison, and the absence of such correlated anomalies at the bulk meteorite scale reflects thermal processing of an initially homogeneous distribution of presolar dust that caused the destruction of thermally fragile, isotopically anomalous presolar components. During these thermal events Mo released from the destructed presolar components may have become volatilized as oxides, while at the same time W was not or only slightly affected. Consequently, while Mo entered the gas phase and was removed from the nebular dust, W was not or only slightly lost (because it was either not volatilized or completely recondensed). The resulting chemical fractionation of Mo and W may have been responsible for generating the elevated W/Mo ratio of leachate L4 (see Section. 5.1.) and would have also caused a decoupling of the Mo and W isotope systematics. The W isotopic composition of the processed dust remained largely unaffected, so that the lack of significant nucleosynthetic W isotope anomalies in bulk meteorites reflects the initially homogeneous distribution of isotopically diverse presolar components in the solar nebula. In contrast, the Mo isotopic composition of the nebular dust was modified, because isotopically anomalous Mo was removed from the dust as volatile Mo oxides. As a result the Mo isotopic composition of the processed nebular dust would be anomalous and complementary to the isotopic composition of the volatilized Mo. The thermal processing, therefore, would have imparted Mo isotope heterogeneity on an initially homogeneous mixture of presolar nebular dust. In this model, the Mo isotope anomalies at the planetary scale would reflect accretion of the planets and meteorite parent bodies from nebular dust that was thermally processed to different degrees.

The IVB iron meteorites are the only group of bulk meteorites for which small nucleosynthetic W isotope anomalies have been reported so far (Qin et al., 2008a; Kruijer et al., 2012). Based on their fractionated siderophile element abundances it was proposed that the formation of the IVB irons involved high temperature volatilization in the solar nebula prior to parent body accretion (Campbell and Humayun, 2005; Walker et al., 2008). It is noteworthy that the nucleosynthetic W isotope anomalies of the IVB irons are smaller than what would be expected from their Mo isotopic anomaly (see Fig. 4b). This together with the evidence for high-temperature volatilization of the IVB precursor material in the solar nebula may reflect the loss of some volatile W oxides together with Mo, which can be achieved under highly oxidizing conditions (Fegley and Palme, 1985). Since Mo is always more volatile than W, a larger fraction of Mo than W was lost, so that the resulting nucleosynthetic W isotope anomaly is smaller than expected from the ε^{183}W–ε^{92}Mo correlation revealed by the Murchison leachates.

The thermal processing must have caused the selective destruction of either at least one *s*-process carrier or, alternatively, a component enriched in *p*- and *r*-process isotopes. As noted earlier, the latter cannot be a specific nucleosynthetic carrier because any nucleosynthetic process is unlikely to produce *p*- and *r*-process isotopes in exactly solar proportions. This component, therefore, most likely represents the homogenized portion of the protosolar nebula (see Section. 4.1). Thermal processing of nebular dust is expected to be most severe close to the Sun, and so the material accreted to the Earth should be more strongly affected than the meteorites. Since Earth is enriched in *s*-process Mo isotopes compared to meteorites (Burkhardt et al., 2011), this would imply that the thermal processing selectively destroyed the homogenized component of the solar nebula, which is enriched in *p*- and *r*-process isotopes. The isotopic signature of this component is preferentially released in the early leaching steps and it is thus conceivable that, in contrast to the acid-resistant *s*-process carriers, these easy leachable carriers also were thermally less stable and were preferentially destroyed. If correct, the Earth would have formed from strongly processed material, consistent with conclusions made based on Ti isotopic data (Trinquier et al., 2009).

6. Comparison to other isotope anomalies

The same acid leachates from Murchison investigated in the present study have also been analyzed for Ca (Chen et al., 2011b), Cr (Papanastassiou et al., 2010) and Os isotopes (Reisberg et al., 2009). Furthermore, isotopic data for Sr, Ba, Sm, Nd, Hf (Qin et al., 2011a), and Zr (Schönbächler et al., 2005) are available for acid leachates from Murchison obtained using protocols similar to those used here. These combined data allow assessing the different processes leading to isotopic anomalies in meteorite components and bulk meteorites.

The isotopic variations in the different leaching steps of Murchison are broadly correlated for all elements heavier than Fe (except Os) in the sense that *s*-process depleted signatures are released in the early leaching steps (L1-3) while the later leaching

steps are characterized by *s*-process enriched isotopic compositions (see Fig. S1 in electronic supplement). The isotopic anomalies in the leachates for these elements are thus likely hosted in common carriers. In contrast, no obvious correlation is observed for Ca, Cr (and Ti) and Mo isotopic anomalies in the leachates (Fig. S1), as expected from the different nucleosynthetic origins of these elements. This indicates that the iron peak elements reside in different carriers than the heavier elements (*e.g.*, nanospinels of supernova origin for ^{54}Cr (Dauphas et al., 2010; Qin et al., 2011b)) and is consistent with the lack of correlated anomalies between these two groups of elements at the bulk meteorite scale (Burkhardt et al., 2011). Based on the observation that ^{46}Ti and ^{50}Ti anomalies are correlated in bulk meteorites but not in acid leachates of primitive chondrites, Trinquier et al. (2009) argued that the Ti (+Cr) isotopic anomalies in bulk meteorites were caused by thermal processing and evaporation of presolar dust. Thus, although Mo and the iron group elements have different nucleosynthetic origins and reside in different carriers, the isotopic heterogeneity observed for these elements at the bulk meteorite scale may have been caused by similar nebular processes.

In contrast to Mo, there are no resolvable nucleosynthetic Os isotope anomalies in bulk meteorites, indicating a homogeneous distribution of different presolar carriers at least for Os (Brandon et al., 2005; Yokoyama et al., 2007; Walker, 2012). Osmium and Mo isotopic anomalies in the acid leachates of Murchison are not well correlated (Fig. S1h). This may indicate that Os resides in different carrier phases than the other heavier elements or, alternatively, that isotopically anomalous Os has been redistributed by aqueous alteration on the chondrite parent bodies (Yokoyama et al., 2011). However, the dominant carrier for *s*-process Os in chondrites seems to be SiC (Brandon et al., 2005; Yokoyama et al., 2007), which also is an important carrier for *s*-process isotopes of other heavy elements. Yokoyama et al. (2010) proposed that the isotopic heterogeneity observed for several elements might reflect the selective removal of certain presolar grains but Os was not affected by this process. This is consistent with the origin of Mo isotopic anomalies in bulk meteorites proposed here (Section. 5.2). Osmium has a higher condensation temperature than Mo and remains highly refractory even under highly oxidizing conditions (Fegley and Palme, 1985), and so would not be affected by the thermal processing that caused the selective removal of a presolar Mo isotope component. As such, the thermal processing model may not only account for the Mo isotopic anomalies in bulk meteorites and the lack of corresponding nucleosynthetic W isotope anomalies, but is also consistent with the lack of any evidence for nucleosynthetic Os isotope anomalies in bulk meteorites.

It is less clear as to whether the alternative model discussed above, mixing of different presolar components with the "normal" solar nebula component characterized by high W/Mo (Section. 5.1.), is compatible with the observed Os isotopic homogeneity at the bulk meteorite scale. During the differential dissolution of Murchison, the majority of Os is released in the first three leach steps (L2 contains ~49% of the Os), while leach step L4 contains only a small fraction of the Os (~2%) (Reisberg et al., 2009). The Os distribution among the different leach steps thus is different from that of W but more similar to that of Mo. We performed the same mixing calculations for Os as described above for Mo and W isotopes. While these calculations successfully reproduce the observed lack of resolvable nucleosynthetic W isotope variations at the bulk meteorite scale (Section. 5.1), they cannot reproduce the constant and terrestrial Os isotopic compositions of bulk meteorites. The reason for this is that unlike for W, the leach fractions with the highest Os/Mo and Os contents have Os isotopic compositions significantly different from the terrestrial composition.

The Mo isotope anomalies in the Murchison leachates are roughly correlated with those in Zr (Fig. S1d), suggesting that Mo and Zr are hosted in the same presolar carriers. Thus, in principle it would be expected that bulk meteorites show nucleosynthetic Zr isotope anomalies similar to those observed for Mo. However, Zr is more refractory than Mo and like Os remains highly refractory under oxidizing conditions. Consequently, Zr should not have been affected by the thermal processing of nebular dust proposed here. However, Akram et al. (2011) reported Zr isotope anomalies for bulk carbonaceous chondrites, but these are most likely controlled by the abundance of CAI (which are characterized by an *r*-excess) and thus not related to the process responsible for generating Mo isotope anomalies in bulk meteorites (which are characterized by an *s*-deficit). Moreover, after correcting the Zr isotope anomalies of carbonaceous chondrites for the presence of CAI, all meteorites seem to have homogeneous Zr isotopic compositions (Akram et al. 2011), as expected in the thermal processing model.

The Mo isotopic anomalies in bulk meteorites correlate with those in Ru exactly as predicted from *s*-process nucleosynthesis theory (Burkhardt et al., 2011; Chen et al., 2010; Dauphas et al., 2004). The Mo–Ru isotope correlation is most readily explained by the heterogeneous distribution of a common *s*-process carrier, supporting models that call upon mixing of distinct presolar components as the dominant process causing isotopic heterogeneity at the bulk meteorite scale. In contrast, the significance of the cosmic Mo–Ru correlation within the framework of the thermal processing model is unclear. Ruthenium has a similar condensation temperature as Mo and is less refractory than W and Os, so that Ru and Mo may have behaved similar during thermal processing of nebular dust. However, Ru forms oxides less readily than Mo, W and even Os (Fegley and Palme, 1985). No Ru isotopic data for acid leachates of primitive chondrites are available yet, but such data will be important for better understanding the origin of the Mo–Ru isotopic correlation among bulk meteorites, and for evaluating the significance of both mixing and thermal processing of presolar dust in generating the correlated Mo and Ru isotope anomalies.

The effects of the thermal processing on isotope anomalies for other elements are more difficult to assess. It is noteworthy, however, that elements characterized by isotopic (near-)homogeneity (*e.g.*, Os, W, Zr, Hf) are all highly refractory (condensation temperature, T_C, ~1700-1800 K), whereas elements that show isotopic heterogeneities at the bulk meteorite scale (*e.g.*, Mo, Ru, Nd) appear to have slightly lower condensation temperatures (T_C ~1500–1600 K). These systematics suggest that condensation temperature may have been one important factor controlling the degree of isotopic heterogeneity for a given element. This would be consistent with the thermal processing model proposed here, but clearly further work is needed to fully understand the isotope systematics of different elements in bulk meteorites.

7. Conclusions

The Mo and W isotopic data for acid leachates of the Murchison chondrite provide important information regarding the early evolution of solar nebula solids and can help to identify the processes that led to planetary-scale isotope heterogeneities for some elements (*e.g.*, Mo, Ru) *and* isotopic homogeneity for others (*e.g.*, Os, W). The correlated Mo and W isotopic anomalies in acid leachates combined with the presence of large Mo isotope variations at the bulk meteorite scale suggests that resolvable nucleosynthetic W isotope anomalies should exist in bulk meteorites. Such large-scale nucleosynthetic W isotope anomalies are not observed, however. The disparate Mo and W isotope

systematics may reflect the heterogeneous distribution of one or several presolar components that were physically mixed with a "normal" solar nebula component characterized by a high W/Mo ratio and near-terrestrial W isotope composition. During mixing W isotope anomalies are largely masked by the dominant normal component, while Mo isotopic anomalies are less diluted and, therefore, present at the bulk meteorite scale. This model implies some sort of nebular process establishing non-solar elemental ratios (*e.g.*, high W/Mo) in the "normal" solar nebula component even for refractory elements. Future studies will need to identify such processes, and should evaluate how mixing of several presolar and nebular components affected the isotopic composition of other elements.

The results in this study indicate that thermal processes within the solar nebula may have been important in generating nucleosynthetic isotope anomalies in bulk meteorites. During thermal processing of a homogeneous mixture of presolar dust, isotopically anomalous Mo may have been preferentially removed as volatile oxides, generating large-scale Mo isotope heterogeneities that are complementary to the isotopic composition of the removed Mo. In contrast, other elements such as Os and W were not or only slightly affected because they were more refractory during the thermal processing and, therefore, their isotopic compositions remained homogeneous at the bulk meteorite scale. The nature and origin of the thermal processing of nebular dust remains elusive, but the peculiar depletions of Mo relative to W and Os in many CAI (Fegley and Palme, 1985) demonstrate that conditions prevailed in the early solar nebula that caused a strong fractionation of Mo from other refractory siderophile elements. The importance of thermal processing of nebular dust for generating isotopic anomalies in other elements will need to be investigated further, as well as the nature of the different carriers responsible for generating isotopic heterogeneities at the bulk meteorite scale. However, at least for Cr and Ti the selective destruction of thermally labile, presolar phases appears to also have been important (Trinquier et al., 2009), suggesting that thermal processing may have been a fundamental process in generating isotopic heterogeneities among bulk meteorites.

Acknowledgments

This research was supported by grants of the Swiss National Science Foundation to T. Kleine (No. 2-77213-08), and of NASA (NNX09AG59G), NSF (EAR-0820807) and a Packard Fellowship to N. Dauphas. This study benefited from constructive discussions with H. Palme, A. Davis and R. Gallino. Constructive and thorough reviews by Liping Qin, an anonymous referee and editor Tim Elliott improved the manuscript and are gratefully acknowledged. The Murchison specimen used in this study was provided by the Field Museum.

Appendix A. Supporting information

Supplementary data associated with this article can be found in the online version at http://dx.doi.org/10.1016/j.epsl.2012.09.048.

References

Akram, W.M., Schönbächler, M., Williams, H.M., Halliday, A.N., 2011. The origin of nucleosynthetic zirconium-96 heterogeneities in the inner solar system. Lunar and Planetary Science Conference 42, #1908.

Andreasen, R., Sharma, M., 2006. Solar nebula heterogeneity in p-process samarium and neodymium isotopes. Science 314, 806–809.

Arlandini, C., Kappeler, F., Wisshak, K., Gallino, R., Lugaro, M., Busso, M., Straniero, O., 1999. Neutron capture in low-mass asymptotic giant branch stars: cross sections and abundance signatures. Astrophys J. 525, 886–900.

Bernatowicz, T., Swan, P., Messenger, S., Walker, R., Amari, S., 2000. Comparative morphology of pristine and chemical-dissolution presolar sic from Murchison. Lunar and Planetary Science Conference 31, #1238.

Brandon, A.D., Humayun, M., Puchtel, I.S., Leya, I., Zolensky, M., 2005. Osmium isotope evidence for an s-process carrier in primitive chondrites. Science 309, 1233–1236.

Burkhardt, C., Kleine, T., Bourdon, B., Palme, H., Zipfel, J., Friedrich, J.M., Ebel, D.S., 2008. Hf–W mineral isochron for Ca, Al-rich inclusions: age of the solar system and the timing of core formation in planetesimals. Geochim. Cosmochim. Acta 72, 6177–6197.

Burkhardt, C., Kleine, T., Dauphas, N., Wieler, R., 2012. Nucleosynthetic tungsten isotope anomalies in acid leachates of the Murchison chondrite: implications for Hf–W chronometry. Astrophysical. J. Lett. 753, L6.

Burkhardt, C., Kleine, T., Oberli, F., Pack, A., Bourdon, B., Wieler, R., 2011. Molybdenum isotope anomalies in meteorites: constraints on solar nebula evolution and origin of the Earth. Earth Planet. Sci. Lett. 312, 390–400.

Campbell, A.J., Humayun, M., 2005. Compositions of group IVB iron meteorites and their parent melt. Geochim. Cosmochim. Acta 69, 4733–4744.

Chen, H., Lee, T., Lee, D., Shen, J.J., Chen, J., 2011a. 48Ca heterogeneity in differentiated meteorites. Astrophysical. J. Lett. 743, L23.

Chen, J.H., Papanastassiou, D.A., Dauphas, N., 2011b. Anomalous Ca isotopic compositions in leachates of Murchison. Lunar Planet. Sci Conf. 42, #2440.

Chen, J.H., Papanastassiou, D.A., Wasserburg, G.J., 2010. Ruthenium endemic isotope effects in chondrites and differentiated meteorites. Geochim. Cosmochim. Acta 74, 3851–3862.

Clayton, D.D., 1982. Cosmic chemical memory – a new astronomy. QJRAS 23, 174.

Dauphas, N., Davis, A.M., Marty, B., Reisberg, L., 2004. The cosmic molybdenum–ruthenium isotope correlation. Earth Planet. Sci. Lett. 226, 465–475.

Dauphas, N., Marty, B., Reisberg, L., 2002a. Molybdenum nucleosynthetic dichotomy revealed in primitive meteorites. Astrophys J. 569, 139–142.

Dauphas, N., Marty, B., Reisberg, L., 2002b. Molybdenum evidence for inherited planetary scale isotope heterogeneity of the protosolar nebula. Astrophys J. 565, 640–644.

Dauphas, N., Remusat, L., Chen, J.H., Roskosz, M., Papanastassiou, D.A., Stodolna, J., Guan, Y., Ma, C., Eiler, J.M., 2010. Neutron-rich chromium isotope anomalies in supernova nanoparticles. Astrophys J. 720, 1577–1591.

Fegley, B., Palme, H., 1985. Evidence for oxidizing conditions in the solar nebula from Mo and W depletions in refractory inclusions in carbonaceous chondrites. Earth Planet. Sci. Lett. 72, 311–326.

Fuji, T., Moynier, F., Telouk, P., Albarede, F., 2006. Mass-independent isotope fractionation of molybdenum and ruthenium and the origin of isotopic anomalies in Murchison. Astrophys J. 647, 106–1516.

Huss, G., 2004. Implications of isotopic anomalies and presolar grains for the formation of the solar system. Antarct. Meteorite Res. 17, 132.

Huss, G.R., Meshik, A.P., Smith, J.B., Hohenberg, C.M., 2003. Presolar diamond, silicon carbide, and graphite in carbonaceous chondrites: implications for thermal processing in the solar nebula. Geochim. Cosmochim. Acta 67, 4823–4848.

Kleine, T., Mezger, K., Munker, C., Palme, H., Bischoff, A., 2004. 182Hf–182W isotope systematics of chondrites, eucrites, and martian meteorites: chronology of core formation and early mantle differentiation in Vesta and Mars. Geochim. Cosmochim. Acta 68, 2935–2946.

Kleine, T., Mezger, K., Palme, H., Scherer, E., Münker, C., 2005. Early core formation in asteroids and late accretion of chondrite parent bodies: evidence from 182Hf–182W in CAIs, metal-rich chondrites, and iron meteorites. Geochim. Cosmochim. Acta 69, 5805–5818.

Kruijer, T.S., Fischer-Gödde, M., Sprung, P., Leya, I., Wieler, R., Kleine, T., 2012. Neutron Capture on platinum and tungsten isotopes in iron meteorites: implications for Hf–W chronometry. Lunar Planet. Sci. Conf. 43, #1529.

Lu, Q., Masuda, A., 1994. The isotopic composition and atomic weight of molybdenum. Int. J. Mass Spectrom. Ion Process. 130, 65–72.

Lugaro, M., Davis, A.M., Gallino, R., Pellin, M.J., Straniero, O., Käppeler, F., 2003. Isotopic compositions of strontium, zirconium, molybdenum, and barium in single presolar SiC grains and asymptotic giant branch stars. Astrophys J. 593, 486–508.

Macke, R.J., Bernatowicz, T., Swan, P., Walker, R.M., Zinner, E., 1999. Non-chemical isolation of silica and presolar SiC from Murchison. Lunar Planet. Sci. Conf. 30, #1435.

Nicolussi, G.K., Pellin, M.J., Lewis, R.S., Davis, A.M., Amari, S., Clayton, R.N., 1998. Molybdenum isotopic composition of individual presolar silicon carbide grains from the Murchison meteorite. Geochim. Cosmochim. Acta 62, 1093–1104.

Niemeyer, S., Lugmair, G.W., 1984. Titanium isotopic anomalies in meteorites. Geochim. Cosmochim. Acta 48, 1401–1416.

Papanastassiou, D.A., Chen, J.H., Dauphas, N., 2010. Anomalous 53Cr and 54Cr and nearly normal Ni in differential dissolution steps of Murchison. Lunar and Planetary Science Conference 41, 2068.

Qin, L., Nittler, L.R., Alexander, C.M.O'D., Wang, J., Stadermann, F.J., Carlson, R.W., 2011b. Extreme 54Cr-rich nano-oxides in the CI chondrite Orgueil – implications for a late supernova injection into the solar system. Geochim. Cosmochim. Acta 75, 629–644.

Qin, L., Carlson, R.W., Alexander, C.M.O'D., 2011a. Correlated nucleosynthetic isotopic variability in Cr, Sr, Ba, Sm, Nd and Hf in Murchison and QUE 97008. Geochim. Cosmochim. Acta 75, 7806–7828.

Qin, L., Dauphas, N., Wadhwa, M., Markowski, A., Gallino, R., Janney, P.E., Bouman, C., 2008a. Tungsten nuclear anomalies in planetesimal cores. Astrophys J. 674, 1234–1241.

Qin, L., Dauphas, N., Wadhwa, M., Masarik, J., Janney, P.E., 2008b. Rapid accretion and differentiation of iron meteorite parent bodies inferred from 182Hf–182W chronometry and thermal modeling. Earth Planet. Sci. Lett. 273, 94–104.

Regelous, M., Elliott, T., Coath, C.D., 2008. Nickel isotope heterogeneity in the early solar system. Earth Planet. Sci. Lett. 272, 330–338.

Reisberg, L., Dauphas, N., Luguet, A., Pearson, D.G., Gallino, R., Zimmermann, C., 2009. Nucleosynthetic osmium isotope anomalies in acid leachates of the Murchison meteorite. Earth Planet. Sci. Lett. 277, 334–344.

Scherstén, A., Elliott, T., Hawkesworth, C., Russell, S., Masarik, J., 2006. Hf–W evidence for rapid differentiation of iron meteorite parent bodies. Earth Planet. Sci. Lett. 241, 530–542.

Schönbächler, M., Rehkämper, M., Fehr, M.A., Halliday, A.N., Hattendorf, B., Günther, D., 2005. Nucleosynthetic zirconium isotope anomalies in acid leachates of carbonaceous chondrites. Geochim. Cosmochim. Acta 69, 5113–5122.

Sprung, P., Scherer, E.E., Upadhyay, D., Leya, I., Mezger, K., 2010. Non-nucleosynthetic heterogeneity in non-radiogenic stable Hf isotopes: implications for early solar system chronology. Earth Planet. Sci. Lett. 295, 1–11.

Trinquier, A., Birck, J.L., Allègre, C.J., 2007. Widespread 54Cr heterogeneity in the inner solar system. Astrophys J. 655, 1179–1185.

Trinquier, A., Elliott, T., Ulfbeck, D., Coath, C., Krot, A.N., Bizzarro, M., 2009. Origin of nucleosynthetic isotope heterogeneity in the solar protoplanetary disk. Science 324, 374–376.

Walker, R.J., McDonough, W.F., Honesto, J., Chabot, N.L., McCoy, T.J., Ash, R.D., Bellucci, J.J., 2008. Modeling fractional crystallization of group IVB iron meteorites. Geochim. Cosmochim. Acta 72, 2198–2216.

Walker, R.J., 2012. Evidence for homogeneous distribution of Osmium in the Protosolar Nebula. Earth Planet. Sci. Lett. 351-352, 36–44.

Yokoyama, T., Alexander, C.M.O., Walker, R.J., 2010. Osmium isotope anomalies in chondrites: results for acid residues and related leachates. Earth Planet. Sci. Lett. 291, 48–59.

Yokoyama, T., Alexander, C.M.O., Walker, R.J., 2011. Assessment of nebular versus parent body processes on presolar components present in chondrites: evidence from osmium isotopes. Earth Planet. Sci. Lett. 305, 115–123.

Yokoyama, T., Rai, V.K., Alexander, C.M.O., Lewis, R.S., Carlson, R.W., Shirey, S.B., Thiemens, M.H., Walker, R.J., 2007. Osmium isotope evidence for uniform distribution of s- and r-process components in the early solar system. Earth Planet. Sci. Lett. 259, 567–580.